UC Santa Barbara

UC Santa Barbara Previously Published Works

Title

An insecticide target in mechanoreceptor neurons

Permalink

https://escholarship.org/uc/item/2jn084nv

Journal

Science Advances, 8(47)

ISSN

2375-2548

Authors

Qiao, Xiaomu
Zhang, Xiaoyu
Zhou, Zhendong
et al.

Publication Date

2022-11-25

DOI

10.1126/sciadv.abq3132

Peer reviewed

eScholarship.org Powered by the California Digital Library
University of California

NEUROSCIENCE

An insecticide target in mechanoreceptor neurons

Xiaomu Qiao[1], Xiaoyu Zhang[1], Zhendong Zhou[1], Lei Guo[1], Weiping Wu[1], Suhan Ma[1], Xinzhong Zhang[2], Craig Montell[3], Jia Huang[1]*

Copyright © 2022 The Authors, some rights reserved; exclusive licensee American Association for the Advancement of Science. No claim to original U.S. Government Works. Distributed under a Creative Commons Attribution NonCommercial License 4.0 (CC BY-NC).

Hundreds of neurotoxic insecticides are currently in use. However, only a few direct targets have been identified. Here, using *Drosophila* and the insecticide flonicamid, we identified nicotinamidase (Naam) as a previous unidentified molecular target for an insecticide. Naam is expressed in chordotonal stretch-receptor neurons, and inhibition of Naam by a metabolite of flonicamid, TFNA-AM (4-trifluoromethylnicotinamide), induces accumulation of substrate nicotinamide and greatly inhibits negative geotaxis. Engineered flies harboring a point mutation in the active site show insecticide resistance and defects in gravity sensing. Bees are resistant to flonicamid because of a gene duplication, resulting in the generation of a TFNA-AM–insensitive Naam. Our results, in combination with the absence of genes encoding Naam in vertebrate genomes, suggest that TFNA-AM and potential species-specific Naam inhibitors could be developed as novel insecticides, anthelmintics, and antimicrobials for agriculture and human health.

INTRODUCTION

Insects are major disease vectors that transmit pathogens that cause diseases afflicting hundreds of millions of people each year (*1*). In addition, insects contribute to worldwide starvation by spreading diseases to domesticated animals and by destroying crops (*2*). To control insect disease vectors and pests, chemical insecticides are used widely, and most (>80% market share) act on the nervous system. Although there are hundreds of neuroactive insecticides, their known molecular targets are restricted to one enzyme, one G protein–coupled receptor, and six ion channels, including the voltage-gated sodium channel (*3*). In addition, two insect transient receptor potential vanilloid (TRPV) channels, Nanchung (Nan) and inactive (Iav), are the only insecticide targets identified over the past three decades (*4*). Three commercial insecticides disrupt insect coordination and inhibit feeding by overstimulating the Nan and Iav channels in chordotonal organs (ChOs) (*4*, *5*), which are specialized mechanoreceptors found at nearly every joint between limbs and body segments (*6*, *7*).

Flonicamid (FL) is a systemic insecticide found in 1992 and is used to control sucking pests like aphids, whiteflies, and thrips (*8*). It also acts selectively on insect ChOs and causes effects reminiscent of the insecticides that target Nan and Iav (*4*, *9*). However, neither FL nor its metabolite TFNA-AM activates heterologously expressed Nan-Iav TRPV channels (*5*). Thus, the molecular target of FL remains unknown.

RESULTS AND DISCUSSION

To identify the direct target for FL, we used a negative geotaxis assay to interrogate candidates using a genetic approach. After tapping down control flies in a vertical tube, nearly all flies that are not exposed to FL climb up to the top half within 10 s (92 ± 2%), and 100% do so within 25 s (0 μM; Fig. 1, A and B). To assay the effects of FL on negative geotaxis, we starved the flies for 10 hours and then allowed them to feed on 10% sucrose combined with different concentrations of the insecticide (20 μM to 2 mM) for 3 hours. FL impaired negative geotaxis in a dose-dependent manner (Fig. 1, A and B). Even at the lowest dose tested (20 μM), only 38 ± 6% reached the top half of the tube within 10 s. A previous study showed that FL may block the insect inward rectifier potassium channel Kir1 and cause toxicity (*10*). However, we found that *Irk1* (*Drosophila* ortholog of Kir1) knockdown flies were still sensitive to FL in climbing assays (fig. S1). Furthermore, Kir1 is mainly expressed in Malpighian tubules and salivary glands but not in ChOs. Therefore, it does not appear to be the molecular target of FL in vivo.

In *Drosophila*, the primary mechanoreceptor that detects gravity is the Johnston's organ (JO)—a chordotonal stretch-receptor organ in the second segment of the antenna with almost 500 sensory neurons (*11*, *12*). Because FL impairs gravitaxis, a protein expressed in the JO might be a direct target for FL. To identify genes enriched in the JO, we compared the RNAs expressed in the second antennal segment of a mutant missing the JO ($ato^1/Df(3R)p^{13}$) (*13*) with their parental controls containing a JO (Fig. 1C). Given that ion channels are the main targets for insecticides, we first focused on the 19 ion channel genes enriched in the JO (fold change of >5). We tested the available null alleles disrupting 12 of these genes. However, all of these mutant flies were still sensitive to FL (table S1).

In addition to ion channels, 47 other genes were highly enriched in the JO, and 31 of them are not characterized functionally (table S2). Among this group is the gene-encoding Naam (nicotinamide amidase or nicotinamidase), which is an enzyme involved in a pathway leading to the biosynthesis of NAD^+ (nicotinamide adenine dinucleotide) (Fig. 1D). Naam is an intriguing candidate target for FL, because its substrate, nicotinamide (NAM) (Fig. 1D), structurally resembles FL (Fig. 1E). Thus, FL might act as an inhibitor of Naam. To test this idea, we expressed and purified recombinant *Drosophila* Naam from *Escherichia coli* and confirmed that it had Naam activity (Fig. 1F). A metabolite of FL, TFNA-AM (4-trifluoromethylnicotinamide), markedly reduced the enzyme activity, while FL or either of two other FL metabolites (TFNA and TFNG) (Fig. 1E) had no significant effect when assayed at 100 μM (Fig. 1G). TFNA-AM potently inhibits Naam with a submicromolar inhibition constant (K_i) (0.72 μM; Fig. 1H). Feeding TFNA-AM to wild-type flies suppressed negative geotaxis at concentrations of ≥20 μM and virtually abolished this activity at 2 mM (Fig. 1I). Together, these data suggest that FL is a

[1]Ministry of Agriculture Key Laboratory of Molecular Biology of Crop Pathogens and Insects, Institute of Insect Sciences, Zhejiang University, Hangzhou 310058, China. [2]Tea Research Institute, Chinese Academy of Agricultural Sciences, Hangzhou 310008, China. [3]Department of Molecular, Cellular, and Developmental Biology and the Neuroscience Research Institute, University of California, Santa Barbara, Santa Barbara, CA 93106, USA.
*Corresponding author. Email: huangj@zju.edu.cn

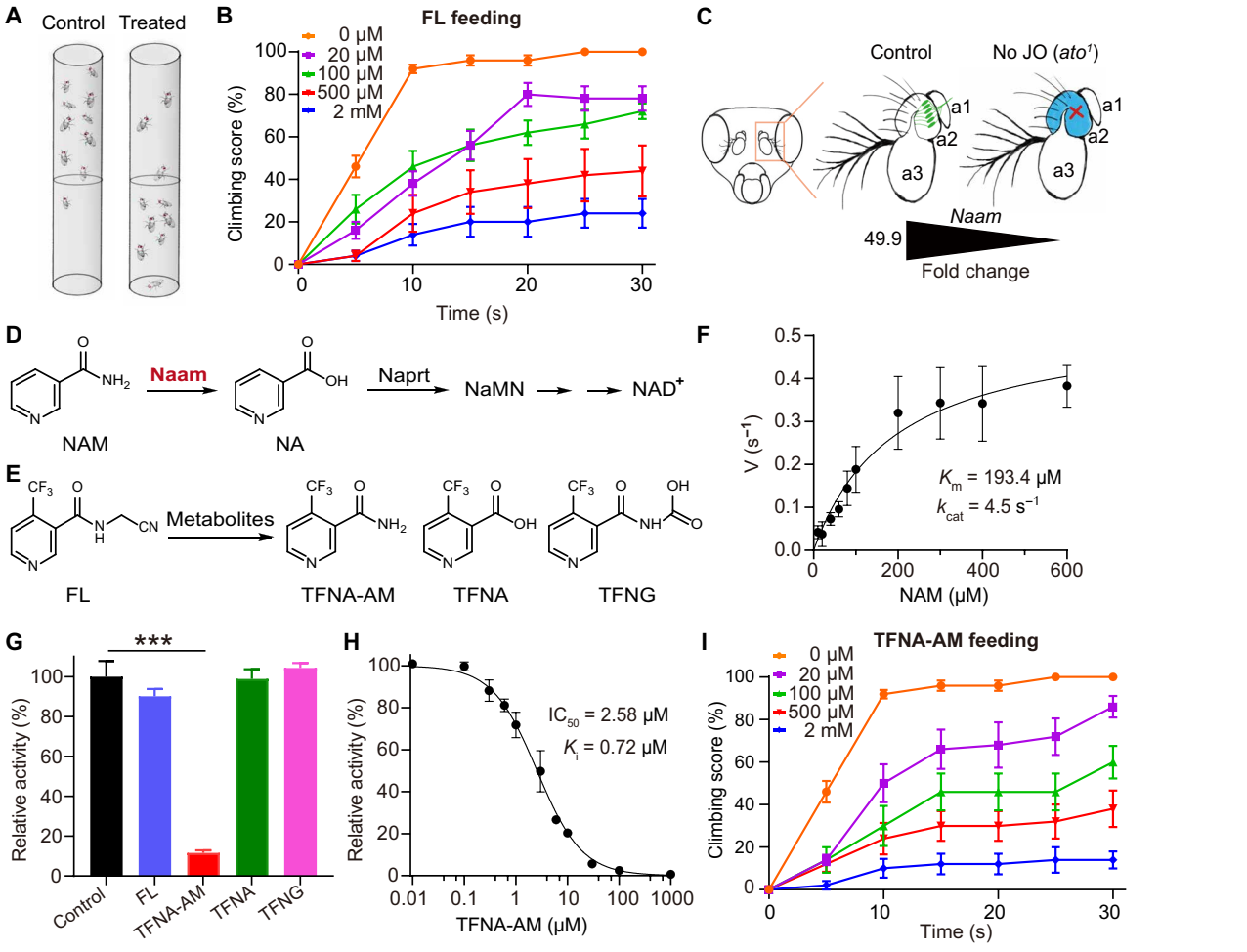

Fig. 1. Identification of Naam as an insecticide target. (**A**) Schematic showing the climbing assay with adult flies. Insecticide-treated flies are impaired in the ability to quickly climb up the vials after they are tapped down. The percentage of flies in the upper half of each vial is the climbing score. (**B**) Flies were fed 10% sucrose mixed with FL at the indicated concentrations for 3 hours, and the climbing scores were determined at 5-s intervals. $n = 5$ (10 flies per assay). (**C**) JO-enriched genes were candidate targets for FL. To perform RNA sequencing, RNA was extracted from the second antennal segments of mutants missing JOs [ato^1/Df(3R)p^{13}] and control flies with JOs [ato^1/TM6B and Df(3R)p^{13}/TM6B]. Illustration of a fly head (left) depicting the localization of the antenna marked in a rectangular box. Sketch of the fly's antenna depicting its second segment harboring the JO (green), which is lost in the mutants (blue). The three antennal segments are indicated as a1, a2, and a3. The *Naam* transcript is markedly reduced in the *ato* mutant. (**D**) NAD^+ salvage pathway in insects. (**E**) Chemical structures of FL and its metabolites. (**F**) Enzymatic activity of purified recombinant Naam. $n = 4$. (**G**) Enzymatic activity of Naam in the presence of 100 μM FL or its metabolites. $n = 3$. (**H**) Inhibition assay of Naam with TFNA-AM. $n = 3$. $^{***}P \leq 0.001$. IC_{50}, median inhibitory concentration. (**I**) Climbing scores (determined at 5-s intervals) of flies fed 10% sucrose combined with TFNA-AM at the indicated concentrations. $n = 5$ (10 flies per assay).

proinsecticide with minimal intrinsic activity, while TFNA-AM is the active metabolite that causes toxicity in vivo.

Given that chordotonal neurons (ChNs) are required for gravitaxis, we set out to determine whether Naam is localized to these neurons. Moreover, the TRPV channels, Nan and Iav, are expressed in ChNs and are activated by NAM (*14*). Thus, inhibition of Naam by TFNA-AM could result in overstimulation of these TRPV channels due to accumulation of NAM. We generated polyclonal antibodies against recombinant *Drosophila* Naam, which detected a protein close to its expected molecular weight (~40 kDa; fig. S2). The Naam antibodies stained the soma, dendrites, and axons of the ChN in the JO (Fig. 2, A and B) and the legs (Fig. 2C). The Naam-positive ChNs in the JO project to the antennal mechanosensory and motor center (AMMC) (Fig. 2D), a brain region associated with mechanosensation (*15*). A previous study produced a *Naam-Gal4* reporter, which used a 950–base pair (bp) region 5′ of the first exon of one transcript, labels JO scolopale cells (*11*). We chose a 3-kb fragment 5′ of the coding sequence to generate a new reporter (*Naam-RB-Gal4*), which specifically labeled ChNs in the JO and legs (Fig. 2, E and F). Expression of this reporter overlapped with most (93.3%) anti–Naam-positive cells (Fig. 2E). Thus, the *Naam-RB-Gal4* appears to reflect the bona fide cellular distribution of *Naam* to a large extent. The targets for two insecticides in ChNs are the *Drosophila* TRPV channels, Nan and Iav (*4*). We used the *iav-Gal4* to drive *UAS-mCD8-GFP* and found that the *iav* reporter and Naam are mainly expressed in distinct populations of ChNs, although a subset of the Naam-positive ChO neurons also expressed the *iav* reporter (27.5 ± 4.4%; Fig. 2, A to D). We also used the *nan-Gal4* to show the relative localization of *nan*-expressing and Naam-positive ChNs, and the results were similar to those with the

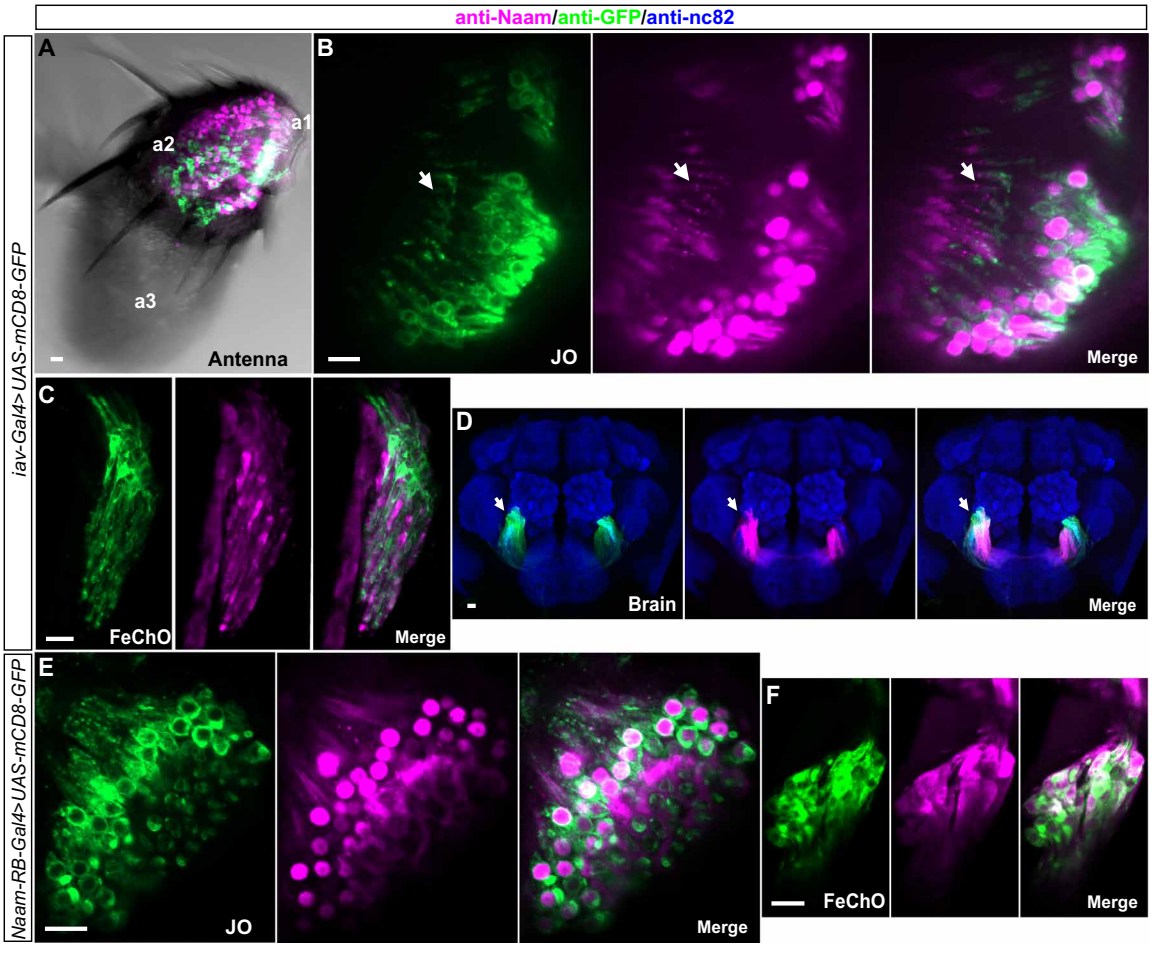

Fig. 2. Localization of Naam in ChNs. (**A**) Double labeling of an antenna with anti-Naam and anti–green fluorescent protein (GFP) in *iav-Gal4;UAS-mCD8-GFP* flies. The three antennal segments are indicated as a1, a2, and a3. All labeling appeared to be in the second antennal segment. The fluorescent image is overlaid on the differential interference contrast image. (**B**) A subset of a JO showing localization of Naam-positive ChNs relative to *iav*-positive ChNs. The white arrow indicates a dendrite. (**C**) Femoral chordotonal organ (FeChO) in an adult foreleg showing localization of Naam-positive ChNs relative to *iav*-positive ChNs. (**D**) Projection patterns of Naam-positive neurons in the AMMC (indicated by arrow) of the brain relative to neurons expressing the *iav* reporter. Counterstaining with nc82 antibody (pan-neuropil marker) is shown in blue. (**E** and **F**) Double labeling of anti-Naam and anti-GFP in JO and FeChO neurons of *Naam-RB-Gal4;UAS-mCD8-GFP* flies. The scale bars represent 10 μM.

iav-Gal4 (fig. S3). Nevertheless, we cannot exclude that the *iav-Gal4* and *nan-Gal4* may not capture the entire endogenous gene expression patterns. We suggest that accumulated NAM may activate the Nan-Iav complex in both an autocrine and paracrine manner.

Next, we set out to test whether inhibition of Naam leads to accumulation of NAM, thereby causing toxicity. We fed the flies 10% sucrose mixed with either 2 mM FL or TFNA-AM for 1 or 3 hours, respectively, before the fly heads were homogenized for high-performance liquid chromatography–mass spectrometry (HPLC-MS) analysis (Fig. 3A). TFNA-AM levels increased gradually when fed with FL (Fig. 3B) but were much higher when fed TFNA-AM directly (Fig. 3C). We did not detect two other FL metabolites TFNA and TFNG in any of the samples tested, presumably because they were below the detection limit. NAM was undetectable without insecticide treatment, increased as the TFNA-AM accumulated (Fig. 3B), and saturated when the flies were fed TFNA-AM for 1 hour (Fig. 3C). Consistent with this observation that feeding TFNA-AM for 1 hour induced much more NAM accumulation than feeding FL, we found that TFNA-AM was more effective than FL in reducing climbing ability after 1 hour of feeding (Fig. 3D). However, the difference was not significant after 3 hours of feeding (Fig. 3D). We then tested whether direct application of NAM would induce a defect in gravitaxis. Feeding high concentrations of NAM (> 10 mM) reduced the climbing scores, while 2 or 5 mM NAM had no significant effect, because it could be metabolized by Naam (fig. S4). Low doses of TFNA-AM (10 or 20 μM) alone also induced negligible effects; however, they significantly synergized the toxicity of NAM, which could not be metabolized efficiently in the presence of the Naam inhibitor (Fig. 3E). Overall, we conclude that the toxicity of TFNA-AM is the consequence of accumulation of NAM in ChNs via inhibition of chordotonal Naam.

To determine whether *Naam* is required to confer toxicity to TFNA-AM, we knocked down *Naam* expression. We initially attempted to use the $Naam^{MI10214}$ null allele, which contains a P element inserted into the coding sequence. However, it is homozygous lethal. Therefore, we used RNA interference (RNAi) to knock down *Naam* expression in ChNs with the *Naam-RB-Gal4* or with the pan-neuronal *elav-Gal4* and tested the effects of TFNA-AM on

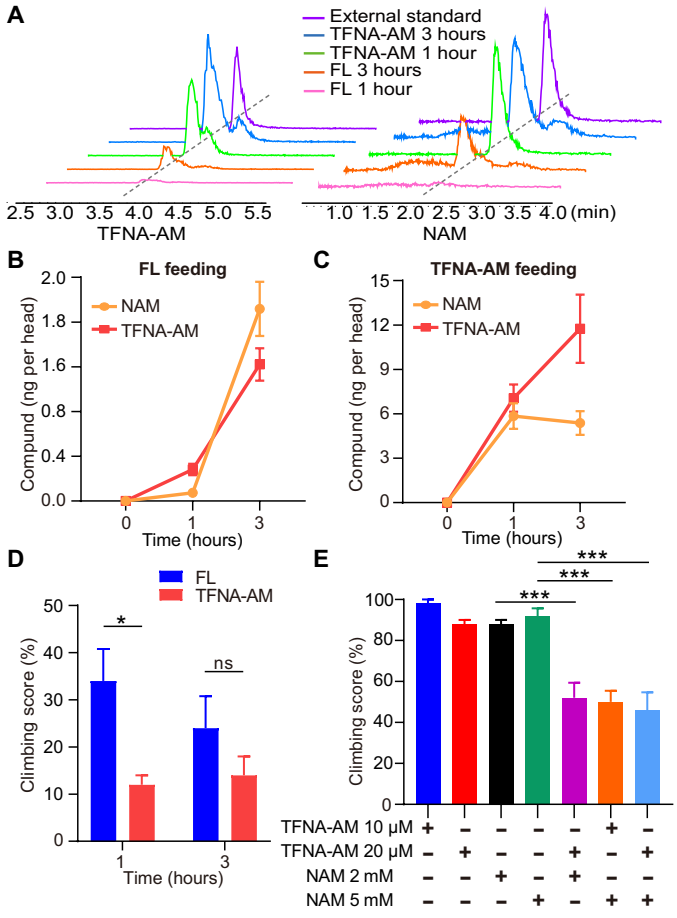

Fig. 3. Inhibition of Naam induced accumulation of NAM, which caused toxicity. (**A**) HPLC-MS traces of TFNA-AM and NAM in adult heads. Flies were fed 10% sucrose mixed with either 2 mM FL or TFNA-AM for 1 or 3 hours, respectively. (**B** and **C**) Levels of TFNA-AM and NAM determined at 0, 1, and 3 hours after feeding 10% sucrose plus either 2 mM FL or TFNA-AM. $n = 3$. (**D**) Climbing scores (at 30 s) of flies fed 10% sucrose plus either 2 mM FL or TFNA-AM for 1 or 3 hours, respectively. $n = 5$ (10 flies per assay). $^*P \leq 0.05$. ns, not significant. (**E**) Climbing scores (at 30 s) of flies fed 10% sucrose plus various concentrations of TFNA-AM and NAM, alone or in combination. $n = 5$ (10 flies per assay). $^{***}P \leq 0.001$.

the climbing assays. We confirmed the knockdown efficiency by immunohistochemistry (fig. S5), real-time quantitative polymerase chain reaction (RT-qPCR) (fig. S6) and Western blotting (fig. S2). All tested flies were normal in climbing assays when treated with 10% sucrose (Fig. 4A). In contrast to control flies, which exhibited very little negative geotaxis after consuming 2 mM TFNA-AM (<15%), knockdown of *Naam* with either the *elav-Gal4* or the *Naam-RB-Gal4* significantly increased the climbing index (68 and 52%, respectively; Fig. 4A). Meanwhile, we found that the *Naam* knockdown flies were still sensitive to the TRPV channel modulator insecticides pymetrozine and pyrifluquinazon (fig. S7), indicating that the resistance is specific to TFNA-AM. These data demonstrate that reducing expression of *Naam* greatly decreased the flies' sensitivity to the insecticide. Knockdown of *Naam* with the *iav-Gal4* had no effect (Fig. 4A), consistent with our finding that many *Naam*-expressing neurons are not colabeled by the *iav-Gal4* (Fig. 2A). Pharmacological inhibition of Naam occurs over a short time window, which is different from transgenic RNAi in which the transcription is greatly suppressed since the early stages of development. Thus, there could be genetic compensation to produce less NAM in *Naam* knockdown flies. Consistent with this hypothesis, NAM levels in *Naam* knockdown flies are almost undetectable before TFNA-AM feeding (fig. S8).

We next investigated the potential binding pocket of TFNA-AM using site-specific mutagenesis. To identify putative amino acid residues that might interact with TFNA-AM, we generated a three-dimensional (3D) structure of Naam by homology modeling using the crystal structure of Naam from *Acinetobacter baumannii* (AbPncA) as the template (*16*). We docked the TFNA-AM ligand into the catalytic site and identified four residues (Asn^{117}, Ala^{265}, Cys^{269}, and Thr^{294}) that were predicted to promote TFNA-AM binding (Fig. 4B). These include Cys^{269}, which is the conserved catalytic residue. To test the requirements for the other three residues for conferring sensitivity of the Naam protein to TFNA-AM, we introduced amino acid substitutions into each residue: N117G, A265E, T294E, and T294F. The T294E and A265E mutants showed 7.5- and 415.7-fold resistance to TFNA-AM, based on increases in the K_i values (Fig. 4C). These mutations also changed the enzyme affinities and turnover numbers (Fig. 4D). The N117G mutant was still sensitive to TFNA-AM (fig. S9A), and the T294F mutation eliminated enzymatic activity (fig. S9B). These results demonstrate that Ala^{265} plays an especially important role in sensitizing Naam to TFNA-AM.

To test whether the A265E amino acid substitution would confer resistance to TFNA-AM, we introduced the point mutation into the *Naam* locus using CRISPR-Cas9–mediated homology-directed repair (HDR). To identify flies likely to harbor the mutation, we maintained flies under TFNA-AM selection (fig. S10) and confirmed the mutation by DNA sequencing (fig. S11). We found that $Naam^{A265E}$ flies took longer time than control flies (>2 min) to climb up to the upper half of the test tube (Figs. 1B and 4E), probably because of their defects in gravity sensing. Ala^{265} is highly conserved, and the A265E substitution caused NAM accumulation in the JO (2.35 ng per head; Fig. 4F) due to its decreased turnover number to ~22% of wild-type Naam (Fig. 4D). Such a level of NAM might slightly activate TRPV channels to induce chordotonal dysfunction in the engineered flies. Of significance, we found that feeding 2 mM TFNA-AM or FL to $Naam^{A265E}$ flies did not impair negative geotaxis (Fig. 4E), and the ingestion of TFNA-AM did not further increase NAM levels (Fig. 4F). In contrast, heterozygous control flies were as sensitive as wild-type flies to TFNA-AM or FL in climbing assays (Fig. 4G). Together, these results indicate that Naam may be the primary molecular target of FL/TFNA-AM in vivo and that a single amino acid replacement is sufficient to cause high resistance due to target site insensitivity.

FL is highly effective for aphids and can also be used to control whiteflies and planthoppers (*17*, *18*). However, it is less toxic to flies and mosquitoes and quite safe for bees and parasitoid wasps (*17*–*20*). Thus, we wondered whether this selectivity of FL is correlated with species-specific differences in sensitivity of their Naam isoforms to TFNA-AM. Therefore, we expressed and purified recombinant Naam from different insect species and performed enzyme assays. We found that the catalytic activities for NAM are similar among different insect Naam homologs (<4.3-fold variation, fig. S12); however, their sensitivities to TFNA-AM are quite different. The aphid Naam showed a K_i value of 0.08 μM, followed by Naam

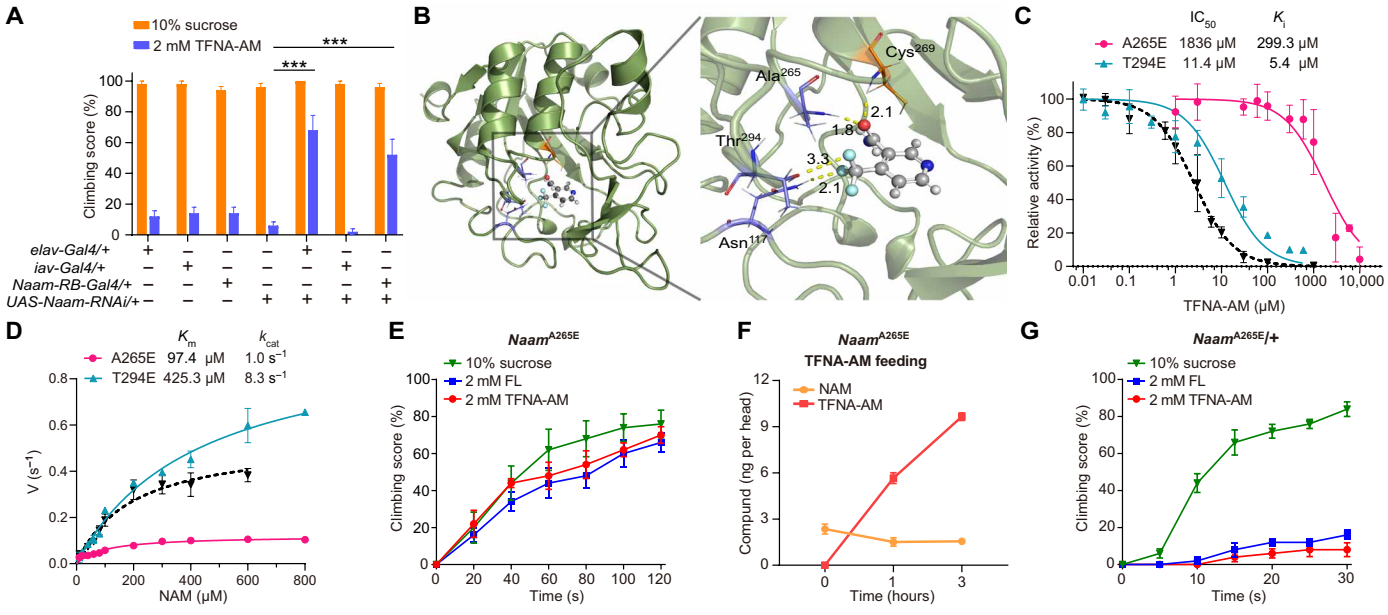

Fig. 4. *Naam* knockdown or a *Naam* point mutation conferred insecticide resistance. (**A**) Climbing scores (at 30 s) of control flies and flies with neuron-specific *Naam* RNAi after feeding with 10% sucrose or 2 mM TFNA-AM for 3 hours. $n = 5$ (10 flies per assay). ***$P \leq 0.001$. (**B**) Homology model of Naam with TFNA-AM (ball-and-stick model) docked into the potential binding pocket. The enlarged view of the TFNA-AM binding site showing putative interactions (distances indicated by the yellow dashes) between amino acid residues (stick model) and TFNA-AM. (**C**) Inhibition assays using purified recombinant Naam mutants and different concentrations of TFNA-AM. The dashed black line shows the results of wild-type Naam. $n = 3$. (**D**) Enzymatic activity of purified recombinant Naam mutants. The dashed black line shows the results of wild-type Naam for comparison. $n = 3$. (**E**) Climbing scores of $Naam^{A265E}$. The flies were fed 10% sucrose combined with either 2 mM FL or TFNA-AM. $n = 5$ (10 flies per assay). (**F**) Levels of TFNA-AM and NAM determined at 0, 1, and 3 hours after feeding 10% sucrose plus 2 mM TFNA-AM in $Naam^{A265E}$ flies. $n = 3$. (**G**) Climbing scores of $Naam^{A265E}$/+ flies fed 10% sucrose combined with either 2 mM FL or TFNA-AM. $n = 5$ (10 flies per assay).

enzymes from the whitefly (0.17 μM), planthopper (0.60 μM), and the mosquito (*Aedes albopictus*), which showed the lowest sensitivity (1.09 μM). This order of TNFA-AM potency is nearly parallel to the toxicities of FL in these species except for the honey bee Naam1, which has a K_i value of 0.81 μM (Fig. 5A and fig. S13).

Bioinformatic analysis of insect genomes reveals that *Naam* is a single-copy gene in most species. However, *Naam* is duplicated (*Naam1* and *Naam2*) in Hymenoptera, such as honey bees and parasitoid wasps (Fig. 5A). We found that the recombinant honey bee Naam2 has similar Michaelis constant (K_m) and catalytic constant k_{cat} values with Naam1 but is resistant to TFNA-AM with a K_i of 16.73 μM (Fig. 5, B and C), which is 21-fold less sensitive than the honey bee Naam1 and 209-fold less sensitive than the aphid Naam. These results indicate that target-site insensitivity is the major mechanism for the resistance of bees to FL. There is a great concern about the negative effects of insecticides on pollinators and natural enemies because most insecticides act on evolutionary conserved ion channels and receptors in insects (*3*). For instance, the severe sublethal effects of neonicotinoids on wild and managed bees caused heavy restrictions on their use in Europe (*21*–*23*). Because the bee-specific Naam2 is pharmacologically different from the canonical Naam, our findings form the conceptual basis to identify safer and more selective insecticides that spare beneficial insects.

The discovery that FL and TFNA-AM inhibit Naam, raised the possibility that chemicals targeting Naam could be used to suppress other disease-causing organisms, such as parasitic worms, which infect ~25% of humans (*24*). Nematodes also contribute to worldwide starvation by destroying crops and infecting domesticated animals (*25*). The nonparasitic nematode, *Caenorhabditis elegans*, provides an effective model for testing anthelmintics (*26*). Therefore, we wondered whether a chemical inhibitor of Naam would serve as an anthelmintic because mutation of the *C. elegans Naam* gene (*pnc-1*) causes uterine cell death, leading to a severe defect in egg production (*27*). In addition to *pnc-1*, *C. elegans* encodes a second *Naam* gene, *pnc-2* (*27*). However, neither PNC-1 nor PNC-2 was sensitive to TFNA-AM (fig. S14). Nicotinaldehyde (NAH) is a general inhibitor of Naam (*28*). Therefore, we tested whether NAH and 4-(trifluoromethyl)nicotinaldehyde (TNAH) suppress the activities of PNC-1 and PNC-2. We found that both chemicals potently inhibit PNC-1 and PNC-2 with comparable K_i values (Fig. 5, D and E). Addition of NAH and TNAH to wild-type nematodes significantly reduced the number of eggs laid, albeit using high concentrations (Fig. 5F). The lower potencies of NAH and TNAH in vivo versus in vitro might be due to the abundant aldehyde oxidases and aldehyde dehydrogenases in animals, which efficiently convert aldehydes to carboxylic acid (*29*). Consistent with this speculation, we found that NAH can also inhibit *Drosophila* Naam with a K_i value of 0.33 μM but had no significant effect on flies in climbing assays even at 5 mM (fig. S15). Overall, our results indicate that rational design of nonaldehyde small molecular inhibitors for worm Naam could be developed as novel anthelmintics.

Previous studies found that Naam is essential for several pathogenic microorganisms such as *Brucella abortus* (causes brucellosis) (*30*), *Leishmania* (causes leishmaniasis) (*31*), and *Borrelia burgdorferi* (causes Lyme disease) (*32*). For instance, the *B. burgdorferi* gene *bbe22*, which encodes a Naam (BbPncA), is necessary for infection of mammals and tick vectors (*32*,*33*). Lyme disease, which is transmitted by ticks infected with *B. burgdorferi*, is the most common

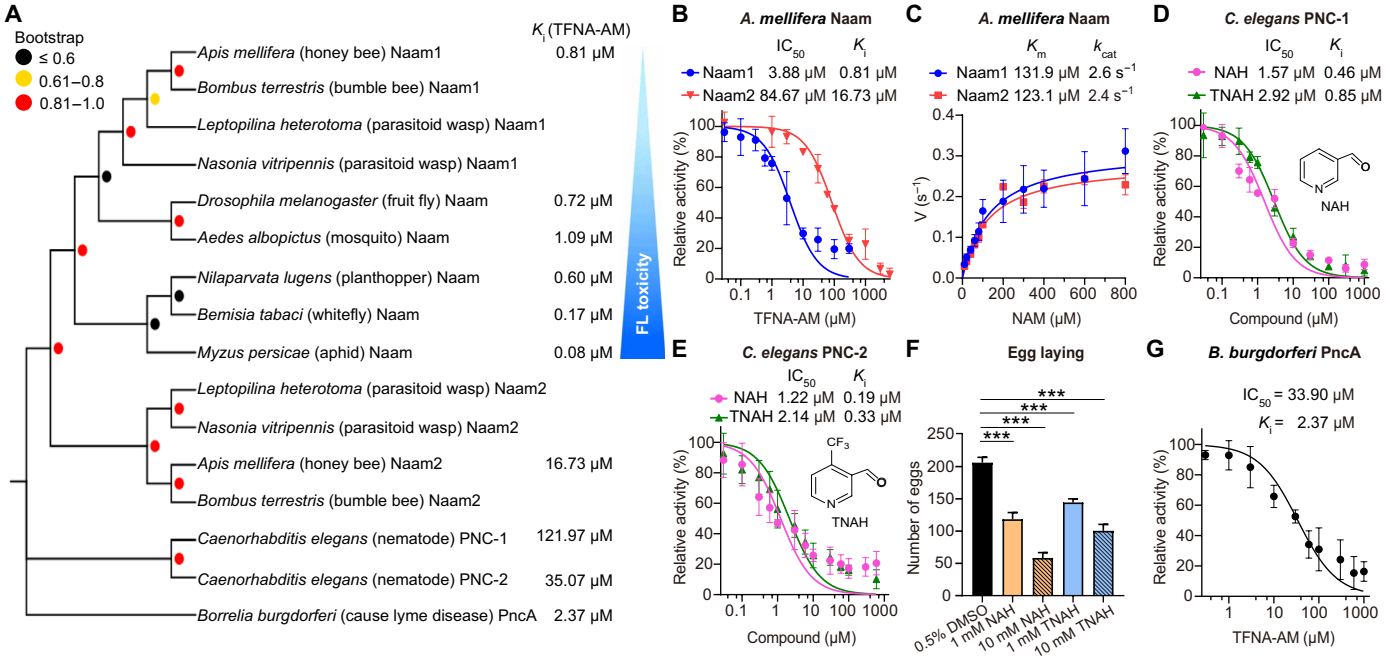

Fig. 5. Naam as a target for selective insecticides and potential anthelmintics and antimicrobials. (**A**) Phylogenetic relationships of Naam from representative insect species and nematodes. The colored dots at the nodes of the branches represent the values of bootstrap support for each branch. *B. burgdorferi* PncA was used as an outgroup. The sequence accession numbers are shown in table S3. The K_i values of TFNA-AM for each Naam are listed on the right, and the blue gradient triangle indicates the toxicity of FL on different insects (*17*–*20*). (**B**) Inhibition assays using purified recombinant Naam1 and Naam2 from the honey bee. $n = 3$. (**C**) Enzymatic activity of purified recombinant Naam1 and Naam2 from the honey bee. $n = 3$ (**D** and **E**) Inhibition of recombinant *C. elegans* PNC-1 and PNC-2 by NAH and TNAH. $n = 3$. (**F**) Eggs laid by control and compound-treated nematodes. $n = 3$. $^{***}P \leq 0.001$. DMSO, dimethyl sulfoxide. (**G**) Inhibition of purified recombinant PncA from *B. burgdorferi* by TFNA-AM. $n = 3$.

vector-borne disease in the United States with an estimated 476,000 annual cases (*34*). Currently, a substantial number of patients treated with antibiotic therapy experience prolonged symptoms including fatigue, pain, joint, and muscle aches, largely due to the formation of drug-tolerant bacteria (*35*). We found that TFNA-AM inhibits recombinant BbPncA with a K_i value of 2.37 μM (Fig. 5G and fig. S16). TFNA-AM causes a low level of toxicity in mammals, with an LD_{50} (median lethal dose) of >2000 mg/kg in mice (*3*). Therefore, TFNA-AM could be a potential drug candidate against antibiotic-tolerant *Borrelia*.

In conclusion, the identification of Naam as a novel target for an effective insecticide that does not target a number of highly beneficial insects, such as bees, offers to lead to the identification of additional Naam inhibitors with even higher potencies. Moreover, tailored design of small molecular inhibitors with high potency against insect Naam isoforms is an especially appealing class of insecticide due to excellent insect-to-mammalian selectivity as a consequence of an absence of genes encoding Naam in vertebrate genomes. Last, the work presented here provides the conceptual basis for developing improved anthelmintics and the use of TFNA-AM and derivatives as antimicrobials.

MATERIALS AND METHODS

Chemicals

FL, TFNA-AM, and pyrifluquinazon were obtained from Wako (Osaka, Japan); NAM, α-ketoglutarate, TFNG, NAH, pymetrozine, and pyrifluquinazon were obtained from Sigma-Aldrich (St. Louis, MO, USA); and NADH (reduced nicotinamide adenine dinucleotide), TFNA, and TNAH were obtained from Bide Pharmatech (Shanghai, China). All reagents were of the highest purity available.

Fly strains

Flies were maintained and reared on conventional cornmeal, agar, and molasses medium at 25° ± 1°C and 60 ± 0% humidity with a photoperiod of 12 hours light:12 hours dark. The following strains with the indicated stock numbers were obtained from the Bloomington Stock Center (Indiana University): $cac^{MI11727}$(#56455), Ih^{f03355} (#85650), $Ca\text{-}\alpha1T^{\Delta135}$ (#68200), $Cngl^{MI03832}$ (#37373), $nAChR\alpha4^{rye}$ (#80692), $Ir94b^{MB02190}$ (#23424), $Task7^{f05437}$ (#18864), $ppk12^{MB11059}$ (#29179), $Naam^{MI10214}$ (#53231), $Naam^{MI04166}$ (#37268), *elav-Gal4* (#8765), *iav-Gal4* (#52273), *nan-Gal4* (#24903), *UAS-mCD8-GFP* (#5137), *UAS-Naam-RNAi* (#44053), *UAS-Irk1-RNAi* (#25823), and *vas-Cas9* (#51323). The following lines were gifts from W. Zhang (Tsinghua University): ato^1/TM6B, *Tb* and Df(3R)p^{13}/TM6B, *Tb* (*36*). All other ion channel mutants (*37*) were gifts from Y. Rao (Peking University). The w^{1118} strain was used as the "wild-type" control for the behavioral assays.

We generated the $Naam^{A265E}$ mutant by CRISPR-Cas9 genome editing with a similar screening strategy as described (*38*). The guide RNA (gRNA) sequence (3 L:19697783 ~ 19697802, GGATATCTATGTGTGCGGAT) was designed using flyCRISPR Target Finder (https://flycrispr.org/target-finder/) and cloned into the pDCC6 plasmid (Addgene, #59985). A 110-bp ssODN (single-strand oligodeoxynucleotide) was synthesized (GenScript, Nanjing, China) as the donor template to replace the targeted genomic region. This ssODN contained three nucleotides changes with two (CC to AA)

conferring the A265E mutation and one synonymous mutation (G to A) to prevent recleavage by Cas9 after incorporation. Both the gRNA plasmid and the ssODN were microinjected into embryos from *vas-Cas9* flies. The crossing and selection scheme is shown in fig. S6.

We generated the *Naam-RB-Gal4* reporter transgene with the phiC31 integration system. To provide a promoter sequence 5′ of *Naam*, we introduced an ~3-kb DNA fragment (3R:19684221 ~ 19687232) and the *Naam* coding sequence into the pBPGAL4.2::VP16Uw plasmid (Addgene, #26228). The construct, which included the *mini-white* gene for selecting transgenic flies, was microinjected into the embryos of *attP40* flies.

Climbing assay

We performed climbing assays as previously reported with slight modifications (*39*). Briefly, about 2- to 4-day-old male flies were collected with CO_2 anesthesia into groups of 10 and then allowed to recover for 2 days. Flies were starved for ~10 hours overnight and fed for 3 hours on either 10% sucrose or 10% sucrose containing the indicated drugs, and the assays were performed between 12:00 p.m. and 1:00 p.m. The climbing tubes (total 180 mm in height and 20 mm in diameter) consisted of two vials connected with transparent tape. The flies were filmed for 30 s with a SONY HDR-CX900E camera. The climbing score (percentage of flies in the upper half of the vial) were determined at 5-s intervals after the flies were tapped down to the bottom of the vials. For $Naam^{A265E}$ mutant flies, the climbing score were determined at 20-s intervals for 120 s. Assays with each genotype and compound were repeated ≥5 times.

Transcriptome sequencing

The second antennal segments of the following lines were dissected on ice and immediately processed to extract total RNA using a standard TRIzol reagent (Thermo Fisher Scientific, Waltham, MA, USA) protocol: (i) ato^1/Df(3R)p^{13}, (ii) ato^1/TM6B, *Tb* (control), and (iii) *Df(3R)*p^{13}*/TM6B, Tb* (control). A complementary DNA (cDNA) library was prepared and sequenced using the Illumina platform (Annoroad Gene Technology, Beijing, China). The mRNA levels were calculated on the basis of the FPKM (fragments per kilobase of transcript per million mapped reads) values. DEGseq was used to identify differentially expressed genes from the RNA sequencing (RNA-seq) data. The transcriptome data were uploaded to the NGDC database with the accession number RPJCA00781 (https://ngdc.cncb.ac.cn/bioproject/browse/PRJCA009781).

Plasmid construction and protein expression

Full-length cDNAs encoding *Drosophila melanogaster* Naam (NP_001262738), *Nilaparvata lugens* Naam (XP_022202218), *Bemisia tabaci* Naam (XP_018907173), *Myzus persicae* Naam (XP_022168570.1), *Apis mellifera* Naam1 (XP_006568548), *A. mellifera* Naam2 (XP_026298838), *A. albopictus* (XP_029723373.1), *B. burgdorferi* PncA (AEK93977.1), *C. elegans* PNC-1 (NP_001367799.1), and PNC-2 (NP_001370171.1) were synthesized and subcloned into the pET-28a(+) expression plasmid (GenScript). All recombinant Naams include a C-terminal His6 tag. The Naam point-mutation (A265E, T294E, N117G, and T294F) plasmids were generated by site-directed mutagenesis by Tsingke Biotechnology (Nanjing, China). The *A. mellifera* Naam1 was subcloned into the pCold-TF vector (Takara, Japan), and the *M. persicae* Naam was subcloned into the pGEX-4 T-2 vector (GenScript). All plasmids were confirmed by DNA sequencing.

In all cases, the Naam-His6 recombinants were induced in *E. coli* BL21(DE3) with 0.2 to 0.4 mM isopropyl-β-D-thiogalactopyranoside (IPTG) once the cell density reached an optical density (OD) of 0.6. After growth for 16 hours at 24°C, the cells were collected and resuspended in the B-PER bacterial protein extraction reagent (Thermo Fisher Scientific, 89822). Cell debris was removed by centrifugation at 16,000*g* for 20 min. The supernatant was applied to Ni–nitrilotriacetic acid (NTA) resin (GenScript, L00250). After washes with wash buffer containing 20 mM tris (pH7.5), 300 mM NaCl, and 10 to 60 mM imidazole, the proteins were eluted from the affinity resin with 250 mM imidazole, 20 mM tris (pH7.5), and 300 mM NaCl. The samples were concentrated using 10- or 30-kDa cutoff centrifugation filters (Millipore) and washed with ≥100 ml of reaction buffer containing 20 mM tris (pH7.5), 150 mM NaCl, and 2 mM $MgCl_2$ by centrifugation at 5000*g*. The concentrated samples were collected and stored at −80°C for future use.

Expression of glutathione *S*-transferase–MpNaam–His6 was induced in BL21(DE3) cells with 0.3 mM IPTG when the cell density reached an OD of 0.6. After growth for 6 hours at 37°C, cells were collected, and MpNaam was purified using glutathione resin (GenScript, L00206). Expression of His6-TF-AmNaam1-His6 was induced in BL21(DE3) cells with 0.2 mM IPTG when the cell density reached an OD of 0.6. After growth for 24 hours at 15°C, cells were collected, and AmNaam1 was purified using Ni-NTA resin as described above.

Generation of Naam antibodies

The immunogen used for generating the *D. melanogaster* Naam polyclonal antibodies was the full-length Naam containing a C-terminal His6 tag. After elution from the Ni-affinity resin, the samples were further purified using anion exchange chromatography (SOURCE 15Q, Cytiva) and size exclusion chromatography (Superdex 200 Increase 10/300 GL, Cytiva). The peak fractions were collected, and Naam protein purity was verified to be >99% by SDS–polyacrylamide gel electrophoresis (SDS-PAGE). The purified sample was shipped to GenScript to generate the rabbit polyclonal antibodies.

Enzyme assay

The Naam activity assays were performed as described (*28*,*40*) with modifications. A typical 200 μl of reaction mixture (pH 7.5, 25°C) contained 1 mM α-ketoglutarate, 500 μM NADH, 3 U of glutamate dehydrogenase (GDH, EC 1.4.1.2; Yuanye Bio-Technology, S10067, Shanghai, China), and different concentrations of NAM. Reactions were initiated by addition of purified Naam to individual wells in an ultraviolet transparent 96-well microplate (Corning, 3635), and the decreasing fluorescence intensity at 340 nm was continuously monitored with a microplate reader (Varioskan Flash, Thermo Fisher Scientific) for a total of 900 s at 15-s intervals. Naam concentrations used were as follows: 120 nM Naam, 25 nM BtNaam, 24 nM NlNaam, 68 nM AmNaam1, 120 nM AmNaam2, 15 nM MpNaam, 120 nM AaNaam, 120 nM BbPncA, 60 nM CePNC-1, and 120 nM CePNC-2. The decrease absorbance of NADH by GDH measured at 340 nm represents the rate of NAM consumption, which reflects Naam activity.

For Naam inhibition measurements, various concentrations of compounds were added to the reaction mixtures. Each 200 μl of reaction mixture (pH 7.5, 25°C) contained 1 mM a-ketoglutarate, 500 μM NADH, 3 U of GDH, and 500 μM NAM. The reactions were initiated by addition of 120 nM Naam to the microplates, and the decreasing fluorescence intensity at 340 nm was continuously

monitored with a microplate reader (Varioskan Flash, Thermo Fisher Scientific) for a total of 900 s at 15-s intervals.

The calculations of the kinetic parameters were performed with GraphPad Prism 9.0. The data were fit to the Michaelis-Menten equation to determine K_m values and fit to the [Inhibitor] versus normalized equation to determine median inhibitory concentration (IC_{50}) values. K_i values were calculated according to the Cheng-Prusoff equation $K_i = IC_{50}/(1 + [s]/K_m)$.

HPLC analysis

Four-day-old and uniform-size adult females were starved for 10 hours and fed 10% sucrose (w/v) containing 2 mM FL, TFNA-AM, or 0.1% dimethyl sulfoxide (DMSO) as the solvent control for 1 or 3 hours. Thirty heads from each group were dissected and homogenized in 200 μl of H_2O and centrifuged through a 0.22 μM filter (Corning, 8160). We compared NAM levels in both dissected second antennal segments and heads in preliminary tests, and there was no significant difference. Therefore, we used head samples in all HPLC experiments. About 20 μl of filtered solution was injected into a 2-ml amber vial for analysis with a Waters UPLC (ultra performance liquid chromatography)–tandem MS system (Waters Corp., Milford, MA, USA), as described previously (*41*).

Western blot analysis

Protein extracts for Western blot analysis were prepared by homogenizing five 5-day-old male flies. Total protein extracts (10 μg) were separated by SDS-PAGE (8 to 16%; GenScript, M00658) and transferred to polyvinylidene difluoride membranes (Millipore, ISEQ00010) using the eBlot L1 wet protein transfer system (GenScript). The membranes were blocked with 5% bovine serum albumin in tris-buffered saline for 1 hour. The following primary antibodies were used: rabbit anti-Naam (1:2000), mouse anti–glyceraldehyde phosphate dehydrogenase (1:5000; Proteintech, 60004-1-Ig).

Immunohistochemistry

Immunohistochemistry was performed as described previously (*42*). The dissected brains and antennas were fixed in 4% polyoxymethylene for 45 min following three washes in 0.3% Triton X-100 phosphate-buffered saline (PBS) (PBST) for 20 min each. The hindlegs were fixed in a 1:1 mixture solution of 16% polyoxymethylene and *n*-heptane for 30 min, following three washes in 0.3% PBST for 20 min each. The samples were then blocked in 5% goat serum for 40 min before being incubated with the primary antibodies in 5% goat serum for ~24 hours at 4°C: rabbit anti-Naam (1:5000) and chicken anti–green fluorescent protein (1:1000; A-10262, Thermo Fisher Scientific). After three washes in 0.3% PBST for 20 min each, the samples were incubated with the secondary antibodies for ~24 hours at 4°C: Alexa Fluor 488 goat anti-chicken (1:1000; A-11039, Thermo Fisher Scientific) and Alexa Fluor 568 goat anti-rabbit (1:1000; A-11011, Thermo Fisher Scientific). The samples were washed and mounted in antifade reagent (S36936, Thermo Fisher Scientific). Both microscopy and image processing were performed using an LSM 800 laser scanning confocal microscope (Zeiss, Germany).

Molecular docking

The molecular docking was performed according to procedures similar to those described (*43*). The Naam model was built on Molecular Operating Environments using the *Acinetobacter baumanii* Naam crystal structure (Protein Data Bank ID: 2wt9) as the homology template. The model was evaluated using Ramachandran plots and the UCLA (University of California, Los Angeles)-DOE (Department of Energy) server. During molecular docking calculations, water molecules were deleted, 3D protonation was added, and the energy of the protein models was minimized using the MOE (Molecular Operating Environment) algorithm with default parameters. The MOE-dock program was used for docking compounds, and energies were minimized. To search for the correct conformations during the calculations, the ligand TFNA-AM was kept flexible. The default parameters were set according to the rigid receptor docking protocol. Thirty conformations containing the docked poses and scored were output at the end of the dock operation. A lower binding free energy in the docking simulation indicates a better binding interaction between the enzyme and the ligand.

Phylogenetic analysis

To identify the orthologs of Naam in different insect species, we searched the National Center for Biotechnology Information non-redundant protein database using BLASTP. We renamed these Naam proteins according to their closest orthologs. All the amino acid sequences were aligned by Clustal X. A neighbor-joining tree was performed by MEGA 11 with default parameters, 1000 bootstrap replications, and substitution with the JTT (Jones-Taylor-Thornton) model and visualized by Evolview (https://evolgenius.info//evolview/).

Egg-laying assay

The N2 Bristol strain of *C. elegans* was maintained at 20°C on nematode growth medium plates seeded with the OP50 strain of *E. coli* under standard conditions. Thirty worms for each group were picked at the early L3 stage and cultured on 6-cm plates at 20°C for 24 hours. M9 buffer (250 μl) containing drugs or DMSO was added to the plates. All plates were sealed with parafilm to prevent evaporation of nicotinaldehydes. Twenty worms for each group were transferred to new plates after 48 hours and were allowed to lay eggs for 90 min at 20°C as described (*44*). At the assay end point, the number of eggs was counted. Each compound with two doses was repeated ≥3 times.

Real-time qPCR

The relative transcription levels of *Naam* in different RNAi and control flies were examined using RT-qPCR performed with a CFX96TM Real-Time PCR System (Bio-Rad, Hercules, USA). Total RNA was isolated with the TRIzol reagent according to the manufacturer's instructions. Residual genomic DNA was removed by RQ1 RNase-Free DNase (Promega, Madison, USA). Total RNA was reverse-transcribed to cDNA with EasyScript First-Strand cDNA Synthesis SuperMix (Transgene, Beijing, China). RT-qPCR with gene-specific primers [*Naam*, 5′-GACCGCCTGAGTCTTGCCGAAT-3′ (forward) and 5′-TCTCGTGTCCTTGCTGCTGTGC-3′ (reverse)] was performed with ChamQ Universal SYBR qPCR Master Mix (Vazyme, Nanjing, China). *RpL32* [ribosomal protein L32, 5′-GACGCTTCAAGGGACAGTATCTG-3′ (forward) and 5′-AAACGCGGTTCTGCATGAG-3′ (reverse)] was used as an internal control. The relative expression of *Naam* was normalized to the reference (*RpL32*) using the $2^{-\Delta\Delta CT}$ method.

Statistical analysis

All statistical calculations were performed using GraphPad Prism 9.0 (San Diego, CA). Data were expressed as the means ± SEMs.

Unpaired Student's *t* tests were used for Fig. 3D. For comparison of three or more sets of data, we performed one-way analysis of variance (ANOVA) and Tukey's multiple comparisons tests.

SUPPLEMENTARY MATERIALS

Supplementary material for this article is available at https://science.org/doi/10.1126/sciadv.abq3132

View/request a protocol for this paper from *Bio-protocol*.

REFERENCES AND NOTES

1. A. L. Wilson, O. Courtenay, L. A. Kelly-Hope, T. W. Scott, W. Takken, S. J. Torr, S. W. Lindsay, The importance of vector control for the control and elimination of vector-borne diseases. *PLOS Negl. Trop. Dis.* **14**, e0007831 (2020).
2. C. A. Deutsch, J. J. Tewksbury, M. Tigchelaar, D. S. Battisti, S. C. Merrill, R. B. Huey, R. L. Naylor, Increase in crop losses to insect pests in a warming climate. *Science* **361**, 916–919 (2018).
3. T. C. Sparks, A. J. Crossthwaite, R. Nauen, S. Banba, D. Cordova, F. Earley, U. Ebbinghaus-Kintscher, S. Fujioka, A. Hirao, D. Karmon, R. Kennedy, T. Nakao, H. J. R. Popham, V. Salgado, G. B. Watson, B. J. Wedel, F. J. Wessels, Insecticides, biologics and nematicides: Updates to IRAC's mode of action classification–A tool for resistance management. *Pestic. Biochem. Physiol.* **167**, 104587 (2020).
4. A. Nesterov, C. Spalthoff, R. Kandasamy, R. Katana, N. B. Rankl, M. Andres, P. Jahde, J. A. Dorsch, L. F. Stam, F. J. Braun, B. Warren, V. L. Salgado, M. C. Gopfert, TRP channels in insect stretch receptors as insecticide targets. *Neuron* **86**, 665–671 (2015).
5. R. Kandasamy, D. London, L. Stam, W. von Deyn, X. Zhao, V. L. Salgado, A. Nesterov, Afidopyropen: New and potent modulator of insect transient receptor potential channels. *Insect Biochem. Mol. Biol.* **84**, 32–39 (2017).
6. J. C. Tuthill, R. I. Wilson, Mechanosensation and adaptive motor control in insects. *Curr. Biol.* **26**, R1022–R1038 (2016).
7. R. G. Kavlie, J. T. Albert, Chordotonal organs. *Curr. Biol.* **23**, R334–R335 (2013).
8. M. Morita, T. Ueda, T. Yoneda, T. Koyanagi, T. Haga, Flonicamid, a novel insecticide with a rapid inhibitory effect on aphid feeding. *Pest Manag. Sci.* **63**, 969–973 (2007).
9. V. L. Salgado, A. Nesterov, R. A. Kandasamy, C. Spalthoff, M. C. Goepfert, Action of insecticides on chordotonal organs. In 13th IUPAC International Congress of Pesticide Chemistry, San Francisco, CA, August 10–14, 2014.
10. M. Ren, J. Niu, B. Hu, Q. Wei, C. Zheng, X. Tian, C. Gao, B. He, K. Dong, J. Su, Block of Kir channels by flonicamid disrupts salivary and renal excretion of insect pests. *Insect Biochem. Mol. Biol.* **99**, 17–26 (2018).
11. A. Kamikouchi, H. K. Inagaki, T. Effertz, O. Hendrich, A. Fiala, M. C. Göpfert, K. Ito, The neural basis of *Drosophila* gravity-sensing and hearing. *Nature* **458**, 165–171 (2009).
12. G. Boekhoff-Falk, D. F. Eberl, The *Drosophila* auditory system. *Wiley Interdiscip. Rev. Dev. Biol.* **3**, 179–191 (2014).
13. P. R. Senthilan, D. Piepenbrock, G. Ovezmyradov, B. Nadrowski, S. Bechstedt, S. Pauls, M. Winkler, W. Mobius, J. Howard, M. C. Gopfert, *Drosophila* auditory organ genes and genetic hearing defects. *Cell* **150**, 1042–1054 (2012).
14. A. Upadhyay, A. Pisupati, T. Jegla, M. Crook, K. J. Mickolajczyk, M. Shorey, L. E. Rohan, K. A. Billings, M. M. Rolls, W. O. Hancock, W. Hanna-Rose, Nicotinamide is an endogenous agonist for a *C. elegans* TRPV OSM-9 and OCR-4 channel. *Nat. Commun.* **7**, 13135 (2016).
15. P. Patella, R. I. Wilson, Functional maps of mechanosensory features in the *Drosophila* brain. *Curr. Biol.* **28**, 1189–1203.e85 (2018).
16. P. K. Fyfe, V. A. Rao, A. Zemla, S. Cameron, W. N. Hunter, Specificity and mechanism of *Acinetobacter baumanii* nicotinamidase: Implications for activation of the front-line tuberculosis drug pyrazinamide. *Angew. Chem. Int. Ed. Engl.* **48**, 9176–9179 (2009).
17. M. Morita, T. Yoneda, N. Akiyoshi, Research and development of a novel insecticide, flonicamid. *J. Pestic. Sci.* **39**, 179–180 (2014).
18. E. Roditakis, N. Fytrou, M. Staurakaki, J. Vontas, A. Tsagkarakou, Activity of flonicamid on the sweet potato whitely *Bemisia tabaci* (Homoptera: Aleyrodidae) and its natural enemies. *Pest Manag. Sci.* **70**, 1460–1467 (2014).
19. Y. C. Zhu, J. Adamczyk, T. Rinderer, J. X. Yao, R. Danka, R. Luttrell, J. Gore, Spray toxicity and risk potential of 42 commonly used formulations of row crop pesticides to adult honey bees (Hymenoptera: Apidae). *J. Econ. Entomol.* **108**, 2640–2647 (2015).
20. J. Taylor-Wells, A. D. Gross, S. Jiang, F. Demares, J. S. Clements, P. R. Carlier, J. R. Bloomquist, Toxicity, mode of action, and synergist potential of flonicamid against mosquitoes. *Pestic. Biochem. Physiol.* **151**, 3–9 (2018).
21. J. D. Crall, C. M. Switzer, R. L. Oppenheimer, A. N. Ford Versypt, B. Dey, A. Brown, M. Eyster, C. Guerin, N. E. Pierce, S. A. Combes, B. L. de Bivort, Neonicotinoid exposure disrupts bumblebee nest behavior, social networks, and thermoregulation. *Science* **362**, 683–686 (2018).
22. B. A. Woodcock, J. M. Bullock, R. F. Shore, M. S. Heard, M. G. Pereira, J. Redhead, L. Ridding, H. Dean, D. Sleep, P. Henrys, J. Peyton, S. Hulmes, L. Hulmes, M. Sarospataki, C. Saure, M. Edwards, E. Genersch, S. Knabe, R. F. Pywell, Country-specific effects of neonicotinoid pesticides on honey bees and wild bees. *Science* **356**, 1393–1395 (2017).
23. N. Tsvetkov, O. Samson-Robert, K. Sood, H. S. Patel, D. A. Malena, P. H. Gajiwala, P. Maciukiewicz, V. Fournier, A. Zayed, Chronic exposure to neonicotinoids reduces honey bee health near corn crops. *Science* **356**, 1395–1397 (2017).
24. P. M. Jourdan, P. H. L. Lamberton, A. Fenwick, D. G. Addiss, Soil-transmitted helminth infections. *Lancet* **391**, 252–265 (2018).
25. J. P. McCarter, Nematology: Terra incognita no more. *Nat. Biotechnol.* **26**, 882–884 (2008).
26. A. R. Burns, G. M. Luciani, G. Musso, R. Bagg, M. Yeo, Y. Zhang, L. Rajendran, J. Glavin, R. Hunter, E. Redman, S. Stasiuk, M. Schertzberg, G. A. McQuibban, C. R. Caffrey, S. R. Cutler, M. Tyers, G. Giaever, C. Nislow, A. G. Fraser, C. A. MacRae, J. Gilleard, P. J. Roy, *Caenorhabditis elegans* is a useful model for anthelmintic discovery. *Nat. Commun.* **6**, 7485 (2015).
27. T. L. Vrablik, L. Huang, S. E. Lange, W. Hanna-Rose, Nicotinamidase modulation of NAD^+ biosynthesis and nicotinamide levels separately affect reproductive development and cell survival in *C. elegans*. *Development* **136**, 3637–3646 (2009).
28. J. B. French, Y. Cen, T. L. Vrablik, P. Xu, E. Allen, W. Hanna-Rose, A. A. Sauve, Characterization of nicotinamidases: Steady state kinetic parameters, classwide inhibition by nicotinaldehydes, and catalytic mechanism. *Biochemistry* **49**, 10421–10439 (2010).
29. A. Ahmed Laskar, H. Younus, Aldehyde toxicity and metabolism: The role of aldehyde dehydrogenases in detoxification, drug resistance and carcinogenesis. *Drug Metab. Rev.* **51**, 42–64 (2019).
30. S. Kim, D. Kurokawa, K. Watanabe, S. Makino, T. Shirahata, M. Watarai, *Brucella abortus* nicotinamidase (PncA) contributes to its intracellular replication and infectivity in mice. *FEMS Microbiol. Lett.* **234**, 289–295 (2004).
31. E. Gazanion, D. Garcia, R. Silvestre, C. Gerard, J. F. Guichou, G. Labesse, M. Seveno, A. Cordeiro-Da-Silva, A. Ouaissi, D. Sereno, B. Vergnes, The *Leishmania* nicotinamidase is essential for NAD^+ production and parasite proliferation. *Mol. Microbiol.* **82**, 21–38 (2011).
32. J. E. Purser, M. B. Lawrenz, M. J. Caimano, J. K. Howell, J. D. Radolf, S. J. Norris, A plasmid-encoded nicotinamidase (PncA) is essential for infectivity of *Borrelia burgdorferi* in a mammalian host. *Mol. Microbiol.* **48**, 753–764 (2003).
33. D. Grimm, K. Tilly, D. M. Bueschel, M. A. Fisher, P. F. Policastro, F. C. Gherardini, T. G. Schwan, P. A. Rosa, Defining plasmids required by *Borrelia burgdorferi* for colonization of tick vector *Ixodes scapularis* (Acari: Ixodidae). *J. Med. Entomol.* **42**, 676–684 (2005).
34. K. J. Kugeler, A. M. Schwartz, M. J. Delorey, P. S. Mead, A. F. Hinckley, Estimating the frequency of Lyme disease diagnoses, United States, 2010–2018. *Emerg. Infect. Dis.* **27**, 616–619 (2021).
35. J. R. Bobe, B. L. Jutras, E. J. Horn, M. E. Embers, A. Bailey, R. L. Moritz, Y. Zhang, M. J. Soloski, R. S. Ostfeld, R. T. Marconi, J. Aucott, A. Ma'ayan, F. Keesing, K. Lewis, C. B. Mamoun, A. W. Rebman, M. E. McClune, E. B. Breitschwerdt, P. J. Reddy, R. Maggi, F. Yang, B. Nemser, A. Ozcan, O. Garner, D. Di Carlo, Z. Ballard, H. A. Joung, A. Garcia-Romeu, R. R. Griffiths, N. Baumgarth, B. A. Fallon, Recent progress in Lyme disease and remaining challenges. *Front. Med.* **8**, 666554 (2021).
36. W. Zhang, Z. Q. Yan, L. Y. Jan, Y. N. Jan, Sound response mediated by the TRP channels NOMPC, NANCHUNG, and INACTIVE in chordotonal organs of *Drosophila* larvae. *Proc. Natl. Acad. Sci. U.S.A.* **110**, 13612–13617 (2013).
37. B. Deng, Q. Li, X. Liu, Y. Cao, B. Li, Y. Qian, R. Xu, R. Mao, E. Zhou, W. Zhang, J. Huang, Y. Rao, Chemoconnectomics: Mapping chemical transmission in *Drosophila*. *Neuron* **101**, 876–893.e4 (2019).
38. W. Lu, Z. Liu, X. Fan, X. Zhang, X. Qiao, J. Huang, Nicotinic acetylcholine receptor modulator insecticides act on diverse receptor subtypes with distinct subunit compositions. *PLOS Genet.* **18**, e1009920 (2022).
39. Y. Sun, L. Liu, Y. Ben-Shahar, J. S. Jacobs, D. F. Eberl, M. J. Welsh, TRPA channels distinguish gravity sensing from hearing in Johnston's organ. *Proc. Natl. Acad. Sci. U.S.A.* **106**, 13606–13611 (2009).
40. D. R. Seiner, S. S. Hegde, J. S. Blanchard, Kinetics and inhibition of nicotinamidase from *Mycobacterium tuberculosis*. *Biochemistry* **49**, 9613–9619 (2010).
41. H. Li, Q. Zhong, X. Wang, F. Luo, L. Zhou, H. Sun, M. Yang, Z. Lou, Z. Chen, X. Zhang, The degradation and metabolism of chlorfluazuron and flonicamid in tea: A risk assessment from tea garden to cup. *Sci. Total Environ.* **754**, 142070 (2021).
42. J. Huang, W. Liu, Y. X. Qi, J. Luo, C. Montell, Neuromodulation of courtship drive through tyramine-responsive neurons in the *Drosophila* Brain. *Curr. Biol.* **26**, 2246–2256 (2016).
43. L. Guo, X. Y. Fan, X. Qiao, C. Montell, J. Huang, An octopamine receptor confers selective toxicity of amitraz on honeybees and *Varroa* mites. *eLife* **10**, (2021).
44. X. Yue, J. Zhao, X. Li, Y. Fan, D. Duan, X. Zhang, W. Zou, Y. Sheng, T. Zhang, Q. Yang, J. Luo, S. Duan, R. Xiao, L. Kang, TMC proteins modulate egg laying and membrane excitability through a background leak conductance in *C. elegans*. *Neuron* **97**, 571–585.e5 (2018).

Acknowledgments: We thank T. Zhou for performing some immunohistochemistry experiments, F. Mao for preparing the samples for RNA-seq, Z. Liu for building the

phylogenetic tree, and D. Chen and L. Kang for help on the nematode assay. **Funding:** This work was supported by the Natural Science Foundation of Zhejiang Province, LR19C140002 (to J.H.); the National Natural Science Foundation of China, 32072496 (to J.H.); the National Natural Science Foundation of China, 31802019 (to X.Q.), the National Institute of Allergy and Infectious Diseases, AI165575 (to C.M.), and the National Institute on Deafness and Other Communication Disorders, DC007864 (to C.M.). **Author contributions:** Conceptualization: X.Q. and J.H. Methodology: X.Q. and Xiaoyu Zhang. Investigation: X.Q., Xiaoyu Zhang, Z.Z., L.G., W.W., S.M., and Xinzhong Zhang. Visualization: X.Q. Supervision: J.H. Writing—original draft: X.Q., C.M., and J.H. Writing—review and editing: X.Q., C.M., and J.H. **Competing interests:** The authors declare that they have no competing interests. **Data and materials availability:** All data needed to evaluate the conclusions in the paper are present in the paper and/or the Supplementary Materials.

Submitted 8 April 2022
Accepted 5 October 2022
Published 23 November 2022
10.1126/sciadv.abq3132